

Journal Pre-proof

Sensitized photooxidation of triclosan pesticide. A kinetic study in presence of vitamin B2

Agustina Reynoso, David Possetto, Eduardo De Gerónimo, Virginia C. Aparicio, José Natera, Walter Massad



PII: S1010-6030(21)00086-1

DOI: <https://doi.org/10.1016/j.jphotochem.2021.113213>

Reference: JPC 113213

To appear in: *Journal of Photochemistry & Photobiology, A: Chemistry*

Received Date: 8 August 2020

Revised Date: 28 January 2021

Accepted Date: 14 February 2021

Please cite this article as: Reynoso A, Possetto D, De Gerónimo E, Aparicio VC, Natera J, Massad W, Sensitized photooxidation of triclosan pesticide. A kinetic study in presence of vitamin B2, *Journal of Photochemistry and amp; Photobiology, A: Chemistry* (2021), doi: <https://doi.org/10.1016/j.jphotochem.2021.113213>

This is a PDF file of an article that has undergone enhancements after acceptance, such as the addition of a cover page and metadata, and formatting for readability, but it is not yet the definitive version of record. This version will undergo additional copyediting, typesetting and review before it is published in its final form, but we are providing this version to give early visibility of the article. Please note that, during the production process, errors may be discovered which could affect the content, and all legal disclaimers that apply to the journal pertain.

© 2020 Published by Elsevier.

Sensitized photooxidation of triclosan pesticide. A kinetic study in presence of vitamin B2

Agustina Reynoso¹, David Possetto², Eduardo De Gerónimo³, Virginia C. Aparicio³, José Natera^{1*} and Walter Massad^{1*}

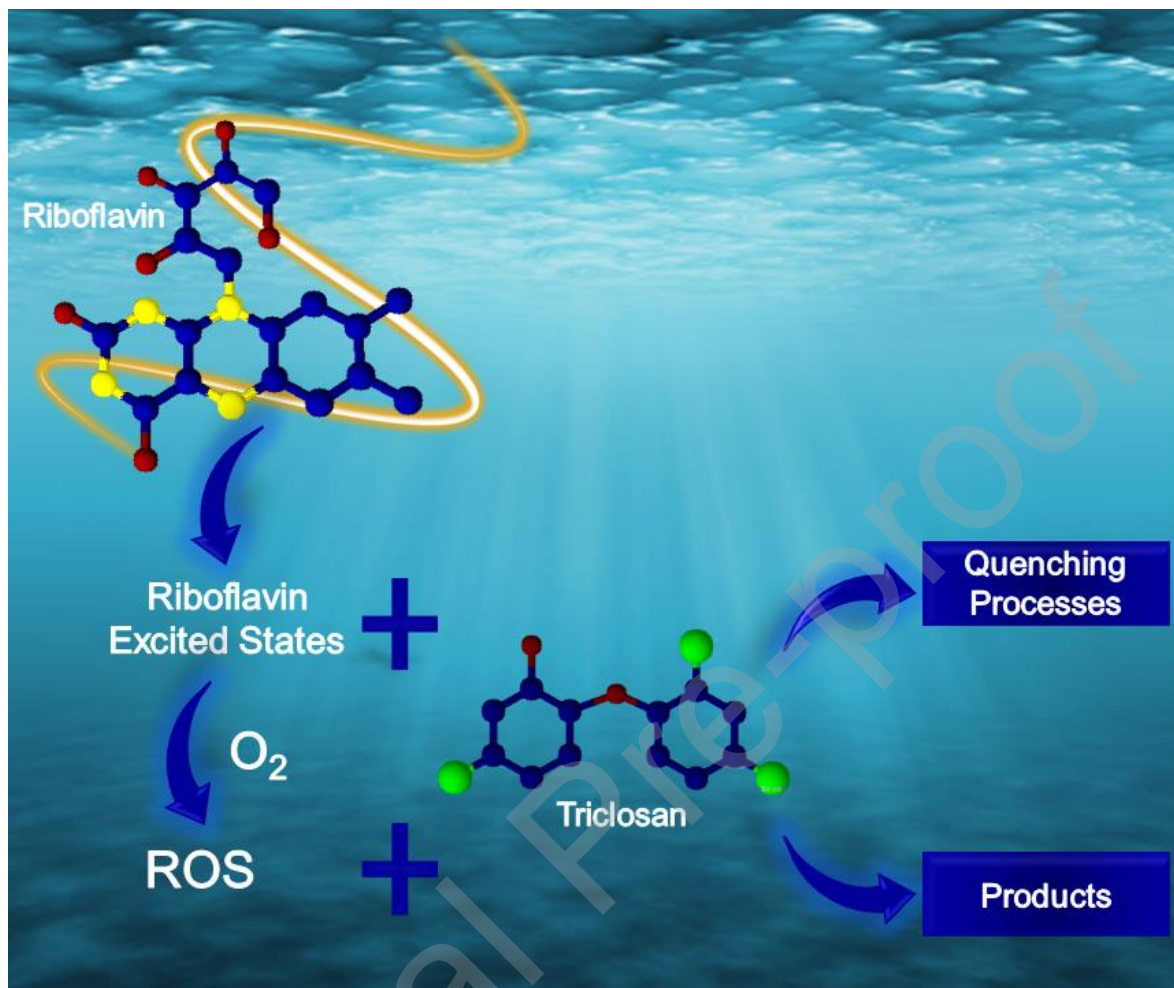
¹*Instituto para el Desarrollo Agroindustrial y de la Salud (IDAS). CONICET – UNRC. Depto. De Química – FCEF-QyN - Universidad Nacional de Río Cuarto*

²*Instituto de Investigaciones en Tecnologías Energéticas y Materiales Avanzados (IITEMA) - CONICET – UNRC. Depto. De Química – FCEF-QyN - Universidad Nacional de Río Cuarto*

³*Instituto Nacional de Tecnología Agropecuaria - Centro Regional Buenos Aires Sur. Estación Experimental Agropecuaria Balcarce*

(*) Corresponding authors: jnatera@exa.unrc.edu.ar, wmassad@exa.unrc.edu.ar

Graphic abstract



Highlights

- Triclosan (TCS) is a broadly-used biocide.
- Vitamin B2 (Rf) under irradiation causes sensitized degradation of Triclosan.
- Triclosan degradation occurs through excited states of Rf and ROS photogenerated.
- TCS is degraded very much rapidly than phenol, a model of water contaminant.

- Photoproducts formed after 30 min of photolysis could be identified.

Abstract

Kinetic and mechanistic aspects of Riboflavin (Rf, vitamin B2)-sensitized photochemical degradation of Triclosan (TCS) have been studied by time-resolved and stationary techniques. TCS is a broadly-used biocide, also employed in a series of industrial products as a multifunctional additive. Rf, in the presence of light and oxygen, generates singlet molecular oxygen ($O_2(^1\Delta_g)$) and superoxide radical anion ($O_2^{\bullet-}$).

Results indicate that TCS quenches the triplet excited state of Rf ($^3Rf^*$), $O_2(^1\Delta_g)$, and $O_2^{\bullet-}$. The reactive rate constant for the interaction TCS- $O_2(^1\Delta_g)$ is 62-fold faster in alkaline medium with respect to pH 7. $O_2^{\bullet-}$ Photosensitized degradation of TCS by Rf was much faster than for phenol, a model pollutant, in similar conditions of pH. Kinetic analysis indicated that the reaction of TCS with $^3Rf^*$ and/or $O_2^{\bullet-}$ is the prevailing oxidative route. Based on the environmental importance of the TCS, the products were determined by UHPLC-MS / MS analysis.

Keywords: Triclosan; Photodegradation; Pesticide; Reactive oxygen species; Vitamin B2;

Journal Pre-proof

1. Introduction

Triclosan (TCS) is a fungicide and broad-spectrum antimicrobial used as a preservative and disinfectant in personal care products, such as soaps, deodorants, antiperspirants, detergents, cosmetics, and anti-microbial creams. Moreover, it is used as an additive in plastics, polymers, and textiles to give these materials antibacterial properties [1–4]. The extensive use of this antimicrobial agent has caused its incorporation into the environment through sewage, thus resulting in a frequent pollutant of terrestrial environments [5].

It is detected in concentrations of parts per trillion in surface waters and parts per million in biosolids. The high concentration of TCS in biosolids and aquatic sediments should not only be attributed to its extensive use, but also to the strong adsorption on organic matter and environmental persistence of this compound [6], thus generating a negative impact on aquatic ecosystems. Other authors have shown that TCS is a pollutant with a long lifetime ($t_{1/2} \sim 8$ days) [7], that it depends on the environmental compartment and the prevailing conditions [8], which can cause potential long-term risks to human health [9,10]. The accumulation of the compound in the ecosystem can lead to resistance from microorganisms, as is the case with antibiotics, and is highly toxic to aquatic organisms [11,12]. The high toxicity of TCS is due to the by-products that are generated during its photodegradation, within which the most important are dioxins [13,14].

TCS is a chlorinated phenoxyphenol with a $pK_a \sim 7.9$ [15]. Photolysis experiments have shown that it is photodegradable in its phenolate form (TCS^-), while it is photostable in its phenolic form [16]. The chemical structures for neutral and ionized species of TCS are shown in Figure 1. Therefore, it is important to

know what happens with TCS in different aquatic environments. , where TCS could be degraded by photosensitized processes. It is well documented that different natural photosensitizers are present in aquatic environments [17–19]. One of the main photosensitizers are humic acids (HA), which are characterized by generating singlet oxygen ($O_2(^1\Delta_g)$) with a quantum yield of 0.04 [20]. Another photosensitizer present in rivers, lakes, and seawater is the vitamin B2 (Riboflavin, Rf) in concentrations 0.1-2 nM [21], which generates $O_2(^1\Delta_g)$ with a quantum yield = 0.47 [22], and the superoxide anion ($O_2^{\cdot-}$) with a quantum yield of 0.009 [23]. Both photosensitizers have been reported as capable of degrading different phenolic pollutants [22,24–29].

All this background shows the importance of investigating the photosensitized degradation of TCS by Rf. For this reason, we perform a kinetic and mechanistic study of this system in different aqueous media. Also, the photoproducts were identified.

<Figure 1>

2. Experimental

2.1. Materials

Triclosan (TCS) 5-Chloro-2-(2,4-dichlorophenoxy)phenol, superoxide dismutase from bovine erythrocytes (SOD), deuterium oxide 99.9% (D_2O), riboflavin (Rf), ammonium acetate, and formic acid were purchased to Sigma Chem. Co. Perinaphthenone (PN), furfuryl alcohol (FFA), monodeuterated

methanol (CH₃OD), and sodium hydroxide were from Aldrich (Milwaukee, WI, USA). Methanol (HPLC quality) was obtained from Sintorgan. All the experiments were carried out at room temperature, using freshly prepared solutions.

2.2. Apparatus and Methods

The solvent in all the experiments in neutral media was a mixture of H₂O-MeOH in equal amounts, to ensure complete solubilization of TCS. Whereas a 0.01 M NaOH aqueous solution was used as basic media.

Absorption spectra were recorded using a Hewlett Packard 8452A diode array spectrophotometer.

2.2.1 Continuous photolysis

Stationary aerobic photolysis of solutions containing TCS and the sensitizer (Rf, A_{445nm} = 0.5) were carried out using a home-made photolyzer [30] with two blue light emitting diodes as light sources (LEDs, λ_{max} 467 nm, polarization current 30 mA, and flux of photons of 40 W/m² for each one). The photon flux of the blue LED was measured with a Luxon SPM-1116SD solar energy meter. The solution to be photolysed was placed in a typical fluorescence cell with an optical path length of 1 cm. The sample was magnetically stirred throughout the experiment guaranteeing homogeneity in the irradiation.

2.2.2 Laser Flash Photolysis Experiments

Laser flash photolysis H₂O-MeOH solutions of Rf 0.05 mM saturated with argon was carried out with equipment previously described [31,32]. To perform the

transient absorption spectra, the signals were adjusted at each wavelength employing a bi-exponential decay function. Lifetime values were shared in the global fit using origin 8.0 software (Origin lab Corp. Northampton, MA, USA). The spectra were obtained by plotting the pre-exponential factors (a_i) for each lifetime using $\Delta A(t) = a_0 \sum_i a_i e^{-t/\tau_i}$ with $i = 2$ [29–35].

2.2.3 O₂-uptake experiments

For the O₂-uptake experiments, the photolysis measurements were carried out in a home-made photolyzer [33] which is provided with a quartz halogen lamp (OSRAM XENOPHOT HPLX 64640, 150w-24 V G35, OSRAM Augsburg, Germany). The light source was equipped with an appropriate cut-off filter according to sensitizer used, 420 nm for Rf experiments, and 320 nm for PN experiments. These cut-off filters were used to remove radiation were TCS absorbs. The light was passed through a water filter and focused into a hermetically sealed reaction cell with a specific oxygen electrode (Orion 97-08). The solutions were continuously stirred. The reactive rate constant of deactivation of O₂(¹Δ_g) by TCS, k_r (see process (11) presented in **Scheme 1**), was determined by the method introduced by Foote and Ching [34]. The PN synthetic sensitizer was used as O₂(¹Δ_g) generator. Assuming the reaction of O₂(¹Δ_g) with the substrate is the only form of oxygen consumption, the ratio of the slope of pseudo first-order plot for oxygen consumption by TCS and by a reference compound (with a known k_{rRef} value), under identical conditions, is equal to k_{rTCS} / k_{rRef} ratio. The reference (Ref) used was FFA, with a reported k_{rRef} value in H₂O-MeOH of $6.2 \times 10^7 \text{ M}^{-1} \text{ s}^{-1}$ [28,29].

In all cases, conversions less than 10% were used to avoid possible interference from the photoproducts.

2.2.4 Time resolved phosphorescence detection of $O_2(^1\Delta_g)$ (TRPD)

The overall rate constant for deactivation of $O_2(^1\Delta_g)$ by TCS ($k_t = k_q + k_{rz}$ processes (12) and (11), in **Scheme 1**) was determined using a previously described method [36]. Briefly, a Nd:YAG laser (Spectron Laser System, SL400) was used as excitation source. The output at 355 nm was used to excite PN, and the $O_2(^1\Delta_g)$ emission at 1270 nm was detected at right angles using an amplified Judson J16 / 8Sp germanium detector, after passing through the appropriate filters. The detector output was coupled to an Agilent Technologies DSO 6012A digital oscilloscope and a personal computer for signal processing. In general, 6-8 shots were averaged, in order to achieve a good signal / noise ratio, from which the decay curve was obtained [37]. D_2O -MeOD, instead of H_2O -MeOH, was used as a solvent to extend the lifetime of $O_2(^1\Delta_g)$ [29]. From a first order fitting of the decay the lifetime of $O_2(^1\Delta_g)$ was evaluated in the presence (τ) and absence (τ_0) of TCS, and the data were plotted as a function of TCS concentration, according to a simple Stern-Volmer treatment.

2.3 TCS degradation products

To obtain the photolysis products of TCS in the presence of Rf, a home-made photoreactor was used, equipped with a merry-go-round equipped with nine LEDs that emitting at 470 nm. In this region, the absorption was due only to Rf. The irradiation was carried out for 300 minutes, taking aliquots every 30 minutes, which

were kept in the dark until further analysis.

The degradation products of TCS were identified by an ultra-performance liquid chromatography-tandem mass spectrometer (UHPLC-MS/MS) analysis, using an ACQUITY UPLC™ system (Waters Corp., Milford, MA, USA) coupled to a Quattro Premier™ XE tandem quadrupole mass spectrometer (Waters, Manchester, UK). Mass Lynx 4.1 software equipped with Quan Lynx software (Waters) was used to control the instruments and to process the data. ACQUITY UPLC equipment consisting of a binary pump, an auto-sampler, and a column heater was used. Chromatographic separation was carried out on a UPLC BEH C18 (1.7µm, 2.1×100 mm; Waters). Solvent **A** was water (0.1 mM NH₄Ac/0.01% formic acid), and solvent **B** was methanol (0.1 mM NH₄Ac/0.01% formic acid). The flow rate was set at 0.3 mL min⁻¹ and the column temperature was 35°C. The chromatography was performed as follows: **B** was 10% in 0-0.5 min, linearly increased to 90% in 0.5-9 min; held at 90% for 9 -12 min and returning to the initial condition in 1 min. An auto-sampler was used to inject 20µL of the samples. The Quattro Premier™ XE tandem quadrupole mass spectrometer was operated in a negative mode with the electrospray-ionization (ESI) source. The operating parameters were optimized under the following conditions: capillary voltage, 3 kV, ion source temperature 120°C, desolvation temperature 450°C, cone gas flow 80 L h⁻¹, desolvation gas flow 800 L h⁻¹ (both gases were nitrogen) and collision gas flow 0.3 mL min⁻¹ (argon gas). Liquid chromatography–mass spectrometry (LC-MS) full-scan was used to select a list of molecular ions whose levels are significantly altered between case and control samples. These molecules are then subjected to precursor-ion (PI) scans to acquire MS/MS data by manually setting the m/z values of the PIs.

A solution of 0.1 mM TCS plus 0.04 mM Rf in MeOH-H₂O mixture was irradiated at $\lambda > 450$ nm in the same device used in the steady-state photolysis experiments previously described in section 2.3. Aliquots to different irradiation time were analyzed by UHPLC-MS / MS to photoproducts determination. The identification of the degradation products formed was carried out from the mass-to-charge ratios, isotopic relation of chlorine atoms, and spectra of the [M-H]⁻ ions produced in the negative electron spray ionization- (ESI⁻) mode. Also, the MS spectra obtained were compared with reference spectra reported by other authors [38,39]. This procedure allows us to guarantee the proposed products structure with 99% confidence.

MZmine 2.13.1 was used for data extraction and analysis of the transformation product [40].

3. Results and Discussion

The results are interpreted and discussed by the mechanism shown in Scheme 1, where Rf is the photosensitizer and TCS is the substrate that can react with Rf electronic excited states (Rf^{*}) or with the reactive oxygen species (ROS) generated from Rf^{*}. This scheme represents a generic photosensitized process in which the absorption of visible light promotes the sensitizer to electronically excited states singlet (¹Rf^{*}) and triplet (³Rf^{*}) (processes (1) and (3)). ³Rf^{*} can transfer an electron to oxygen in its ground state generating the superoxide radical anion species (O₂^{•-}) (process (7)) or transfer energy to it generating the singlet oxygen species (O₂(¹Δ_g)) (process (8)). The latter can decompose by collision with solvent

molecules (process (10)) or it can interact chemically (process (11)) or physically (process (12)) with the photooxidizable substrate.

3.1 Photosensitized degradation

The experiments were performed at pH conditions where the neutral form of TCS is the main species (Figure 1). Spectral changes were observed in a difference spectra of an irradiated ($\lambda > 450$ nm) solution of 0.035 mM Rf plus 0.1 mM TCS vs 0.035 mM Rf in H₂O–MeOH (Figure 2), a region where TCS does not absorb (see figure S1 with the absorption spectrum of Rf for comparative purposes). The time evolution of the absorption spectrum was evaluated in air (Figure 2, main) and inert atmosphere (Figure 2, inset), to discern the oxygen participation in the photosensitized process. The differences between the spectra shown in Figure 2 and inset A of Figure 2, might indicate that the photodegradation of TCS eventually proceeds by different mechanisms. The effect of O₂ participation in the mechanism is corroborated in the Inset B of Figure 2, where it shows the differences in the changes observed at 280 nm, at the maximum of TCS absorption, in the two different conditions. Therefore, in absence of oxygen, spectral changes may be a consequence of the interaction of TCS with ^{*}Rf, whereas those in air equilibrated solution should be the result of possible reactions of TCS with ROS generated from the interaction of ³Rf* and O₂.

<Figure 2>

3.2 The interaction of TCS with electronically excited states of Rf

Since the results obtained in steady-state photolysis experiments might indicate the interaction between TCS and the electronic excited states of the sensitizer, quenching of $^3\text{Rf}^*$ by TCS was investigated.

The quenching of $^1\text{Rf}^*$ was not taken into account, because at the TCS concentrations used in this work, (< 1 mM) the excited singlet of Rf (lifetime 4.5 ns [41]) cannot be intercepted by the quencher.

Therefore, the reaction between the TCS and $^3\text{Rf}^*$, (process (9)), is the most likely explanation for the behavior observed in stationary photosensitization experiments in the absence of oxygen.

<Scheme 1>

The interaction $^3\text{Rf}^*$ -TCS was studied through laser flash photolysis experiments in Ar-saturated H_2O -MeOH solutions. The presence of TCS in the mM concentration range neatly decreases $^3\text{Rf}^*$ lifetime demonstrating the interaction between them. A Stern-Volmer treatment was done at 670 nm, where only $^3\text{Rf}^*$ absorbs. Equation 1 was used to determine the bimolecular rate constant (3k_q) for the quenching of $^3\text{Rf}^*$ by TCS (process (9)).

$$^3\tau / ^3\tau_0 = 1 + ^3k_q [TCS] \quad (\text{eq. 1})$$

where $^3\tau$ and $^3\tau_0$ are the experimentally determined lifetimes of $^3\text{Rf}^*$ in the presence and the absence of TCS, respectively. From the slope of plot $^3\tau / ^3\tau_0$ vs [TCS] was possible to obtain the value of 3k_q (Figure 3, inset). $^3\text{Rf}^*$ quenching yielded a value of $^3k_q = (0.58 \pm 0.04) \times 10^9 \text{ M}^{-1}\text{s}^{-1}$. This value is similar to the reported bimolecular rate

constant for phenol quenching of $^3\text{Rf}^*$ (Table 1). TCS has a phenolic moiety in its structure, which may explain this similarity. Furthermore, this result is significant considering that phenol is considered a paradigmatic water-contaminant model compound.

<Table 1>

In the absence of TCS, the transient absorption spectrum of Rf measured is similar to that previously reported (see Figure S2) [22,42]. The spectrum at 1 μs after the laser pulse presents two a typical maxima, at 680 nm and 310 nm, attributed to $^3\text{Rf}^*$ absorption spectrum [22]. Whereas at 180 μs the spectrum shows a wide band between 500 and 600 nm, with a maximum of 510 nm which can be assigned to the radical RfH^\bullet absorption. RfH^\bullet is formed by the triplet-triplet annihilation given the cation ($\text{Rf}^{+\bullet}$) and anion ($\text{Rf}^{-\bullet}$) radicals of Rf (process (5)), followed by protonation of $\text{Rf}^{-\bullet}$ to produce the neutral radical of Rf (process (14) in scheme 1). This acid-base equilibrium has a reported $\text{pK}_a = 8.3$ [22].

To achieve a better signal-to-noise ratio of the transient spectra, and considering that $^3\text{Rf}^*$ and RfH^\bullet are the principal contributing species, the global fitting method [31] was used for the data analysis. Figure 3 shows the decay-associated spectra of $^3\text{Rf}^*$ and RfH^\bullet obtained using a biexponential decay for each decay. The values obtained from the fitting were $\tau_1 = 32 \mu\text{s}$ and $\tau_2 = 490 \mu\text{s}$. The lifetime measured and decay-associated spectrum for τ_1 agrees with the one

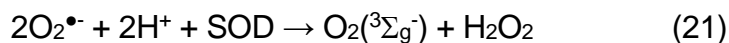
attributed to the $^3\text{Rf}^*$ [29,43] (Figure 3, inset) as long as the spectrum associated with τ_2 is attributed to the species RfH^* [29].

Figure S3 shown, the transient absorption spectrum of a solution of Rf (Abs 0.32 at 355 nm) + 0.38 mM TCS (95% $^3\text{Rf}^*$ quenched by the TCS). In the Figure S3 no new bands were observed with respect to Figure S2. $^3\text{Rf}^*$ Therefore, a global fit with two exponential decays associated to $^3\text{Rf}^*$ and RfH^* were used for the data fitting. The associated spectrum attributed to $^3\text{Rf}^*$ has a lifetime of $\tau_1 = 5.6 \mu\text{s}$ and matches with that obtained for $^3\text{Rf}^*$ in the absence of TCS. While an increase in the absorption band attributed to RfH^* ($\tau_2 = 280 \mu\text{s}$) was observed. When it is compared to the spectrum obtained in the absence of TCS. The increase of the $[\text{RfH}^*]$ in the presence of TCS may be attributed to an electron transfer reaction from TCS to $^3\text{Rf}^*$ (processes (9) and (14) in scheme 1).

3.3 The interaction of TCS with $\text{O}_2^{\bullet-}$

To evaluate the possible participation of the superoxide anion in the photodegradation process (process (19)), rates of oxygen uptake were evaluated, irradiating H_2O – MeOH solutions of 0.03 mM Rf plus 0.1 mM TCS. These experiments were made in the absence and the presence of the enzyme superoxide dismutase (SOD), an $\text{O}_2^{\bullet-}$ -scavenger. SOD catalyzes the dismutation of $\text{O}_2^{\bullet-}$ (process (21)) and has been utilized as a quencher of $\text{O}_2^{\bullet-}$ -mediated photooxidation in similar concentration to those employed in other works [44,45]. Figure S4 shows that the addition of SOD generates an approximately a 40 percent decrease in the

rate of oxygen uptake of TCS, which evidences the participation of $O_2^{\bullet-}$ in the photodegradation of TCS.



3.4 The interaction of TCS with $O_2(^1\Delta_g)$

Numerous authors have reported that the reaction between $O_2(^1\Delta_g)$ and phenolic compounds depends on the degree of ionization of the hydroxyl groups in the molecule [30,46]. Thus, the interaction TCS- $O_2(^1\Delta_g)$ was evaluated in two different media: MeOH-H₂O 1:1 v/v and 0.01 M NaOH aqueous solution, to ensure the presence of the neutral and ionized form of TCS, respectively.

Since Rf photolyzes very easily at pH > 9 [47], the well-known $O_2(^1\Delta_g)$ sensitizer PN was employed instead of the vitamin [48]. PN generates $O_2(^1\Delta_g)$ with a quantum yield of 1 in ethanol [30,49].

The reactive rate constant k_r (processes (11)) was determined by monitoring oxygen uptake upon photo-irradiation of PN-TCS mixtures, through an already described actinometric method [50] using FFA as a reference compound. The k_r values were graphically determined (Inset A, Figure 4) in MeOH-H₂O, 1:1 v/v ($k_r = (0.13 \pm 0.02) \times 10^7 \text{ M}^{-1}\text{s}^{-1}$) and in water at pH 12 ($k_r = (8.04 \pm 0.01) \times 10^7 \text{ M}^{-1}\text{s}^{-1}$) in the presence of PN as a photosensitizer. The results are summarized in Table 1. These differences in k_r values may be due to the ionization of TCS phenolic moiety in water at pH 12. Comparative bibliographic data for phenol is also shown in Table

1, where is observed that the ionized species are more reactive against $O_2(^1\Delta_g)$ than the neutral species.

Figure 4 shows that the presence of sub-mM TCS quenches the $O_2(^1\Delta_g)$ phosphorescence emission. These results unambiguously demonstrate the existence of the interaction between the specific ROS and TCS, via reactive (k_r , process (11)) and/or physical quenching (k_q , process (12)). These possible $O_2(^1\Delta_g)$ deactivation processes were studied in detail as described below.

To investigate the different reactivity towards singlet oxygen of neutral TCS and its ionized form, $O_2(^1\Delta_g)$ quenching experiments were carried out in MeOD/D₂O and D₂O plus 0.01 M NaOH. A lifetime of 37 μ s was obtained for $O_2(^1\Delta_g)$ in D₂O-MeOD and 53 μ s in D₂O in the presence of 0.01 M NaOH in the absence of the quenchers. Rate constants were determined by the TRPD method. The $k_t(k_r + k_q)$ value does not depend on the type of sensitizer or potential interactions of the substrates with excited states of the sensitizer.

The k_t values showed in table 1 indicate dependence with the ionization grade of TCS. For TCS⁻, k_t is 30-fold faster than for neutral TCS. However, in the case of phenolate, k_t is 191-fold faster than phenol. Therefore, the ionization grade has a minor effect in the reactivity of TCS when is compared to phenol. OH-ionization in OH-aromatic compounds produces an enhancement in the electron-donor ability of the compound and, hence, an increase in its $O_2(^1\Delta_g)$ quenching ability. The mechanism involves an intermediate complex possessing charge-transfer character extensively studied [46,51], which depends on the position of the substituents.

Another observation about the results obtained is that the values of the kinetic constant for TCS were higher than for phenol.

However, the values of k_r determined were relatively lower that respect to k_t , this would indicate that TCS interact with $O_2(^1\Delta_g)$ mostly by a physical quenching process (process (12)). The k_r/k_t ratios in Table 1 represent a measure of the efficiency of the degradation pathway *via* reaction with $O_2(^1\Delta_g)$. When the k_r/k_t is ~ 1 indicates high effectiveness in the $O_2(^1\Delta_g)$ -mediated degradation. Table 1 shows that k_r and the ratio k_r/k_t also increases in basic medium.

According, to the low values obtained from the ratio k_r/k_t (table 1), this would indicate that most of the deactivation mechanisms of $O_2(^1\Delta_g)$ proceed by a physical pathway and that even, under competitive conditions favorable to process (11), the process reactive path that involves $O_2(^1\Delta_g)$ can constitute only a minor contribution to the whole mechanism of Rf-sensitized photooxidation of TCS.

The comparison of the quenching rate constant for the reaction of TCS with $^3Rf^*$ ($^3k_q = 0.58 \times 10^9 \text{ M}^{-1}\text{s}^{-1}$) or $O_2(^1\Delta_g)$ ($k_r = 0.13 \times 10^7 \text{ M}^{-1}\text{s}^{-1}$), indicates that the oxidation of TCS mainly implies the participation of $^3Rf^*$.

3q

<Figure 4>

3.4 Feasibility of TCS photooxidation

The formation of RfH^\bullet (processes (9) and (14)), detected by laser flash photolysis (Figure 3), is an indication that there is an electron transfer reaction from

TCS to $^3\text{Rf}^*$. From a thermodynamic point of view, the possibility of the electron transfer process between TCS and Rf is evaluable through the Gibbs free energy change for an electron transfer process [52]:

$$\Delta_{\text{ET}}G_0 = E_{O(\text{TCS}/\text{TCS}^+)} - E_{O(\text{Rf}/\text{Rf}^{\cdot-})} - E_{\text{Rf}^*} + C. \quad (\text{eq. 2})$$

Where the electrode potential of the electron donor, $E_{O(\text{TCS}/\text{TCS}^+)} = 0.68 \text{ V}$ at $\text{pH} = 7$ [53], the Rf data has been previously reported: $E_{O(\text{Rf}/\text{Rf}^{\cdot-})} = 0.80 \text{ V}$ is the standard electrode potential of the acceptor; $E_{\text{Rf}^*} = (2.17 \text{ eV})$ is the $^3\text{Rf}^{\cdot-}$ energy, and the coulombic energy term $C = 0.06 \text{ V}$ [49]. From eq (2) a value of $\Delta_{\text{ET}}G_0 = -0.78 \text{ eV}$ results which constitutes an evidence for the operability of process (8).

As a consequence, the species $\text{O}_2^{\cdot-}$ could be formed through processes (13)-(16) provided that process (19) is kinetically competitive with $\text{O}_2(^1\Delta_g)$ generation step (process (8), k_{ET}). Since $^3k_q = 0.58 \times 10^9 \text{ M}^{-1}\text{s}^{-1}$ for the TCS and $k_{\text{ET}} = 9.5 \times 10^8 \text{ M}^{-1}\text{s}^{-1}$ in MeOH-H₂O (1:1, v/v) (i.e., 1/9 of the diffusional value) [54], it can be inferred that, for the same concentrations of TCS and dissolved $\text{O}_2(^3\Sigma_g^-)$, the rate value for the generation of both $\text{RfH}^{\cdot-}$ -the initial $\text{O}_2^{\cdot-}$ precursor- is almost equal than the corresponding one for $\text{O}_2(^1\Delta_g)$. This finding, in addition to the relatively low k_r value exhibited by TCS, situates the $\text{O}_2(^1\Delta_g)$ -oxidative pathway in a secondary level with respect to the $\text{O}_2^{\cdot-}$ mediated oxidation, under Rf photosensitization.

3.5 Photooxidation products

According to our knowledge, we have not found a report on the Rf-sensitized photooxidation of TCS and their potential photoproducts. To elucidate

the nature of TCS photoproducts, UHPLC-MS / MS experiments were carried out. The obtained chromatograms reveal that TCS is partially degraded after 30 min of irradiation. Moreover, it was possible to identify some of the possible products of degradation at different irradiation times. Figure S5 shows the mass spectra obtained by UHPLC-MS / MS to the different retention times. The chemical structures assigned to the products obtained and their different retention times are shown in Table 2. At the end of the photolysis (300 min), four different products were found, these products are similar to those originated from typical oxidation and/or dimerization reactions of substrates with phenolic groups [29,55,56].

<Table 2>

The exposed results lead to propose that the products come from the electron transfer reaction between the riboflavin sensitizer and the contaminant, originating the radical ionic species. Moreover, the radical anion formed from Rf, in the presence of proton donor solvents and the presence of oxygen, will form different reactive species, which may be reacted with molecular TCS to give different oxidation products (see scheme 1 with the proposed mechanism for TCS degradation).

As can be seen from table 2, hydroxylation of the aromatic ring, it is likely to lead to the formation of monohydroxy triclosan. This may be followed by typical fragmentation of the ether bond [29,56,57] and other species, such as chlorohydroquinone, dichlorocatechol, and dichlorophenol are formed.

5. Conclusions

According to the experimental results, in the photosensitized degradation of TCS by Rf interacts with $O_2(^1\Delta_g)$ and the $O_2^{\cdot-}$. The ROS are generated in situ through energy transfer and electron transfer processes by the interaction of $^3Rf^*$ with $O_2(^3\Sigma_g^-)$ and TCS. The reaction between TCS and $O_2(^1\Delta_g)$ occurs principally through a physical process. Hence, the overall Rf-sensitized photooxidation process seems to be mainly by the reaction with the $^3Rf^*$ and the $O_2^{\cdot-}$.

It was possible to identify the products of the photosensitized degradation of TCS by Rf after 30 minutes of reaction. Unlike other processes, in this case, dioxin formation was not observed between the products.

The complexity and variability of natural waters make it difficult to directly extrapolate our results. However, the presence of the natural photosensitizer Rf and the $O_2^{\cdot-}$ generated from $^3Rf^*$ (among other sources) makes the degradation of the TCS a matter of time in surface waters where solar radiation arrives.

Author Contributions

- Agustina Reynoso and David Possetto conducted the experiments.
- Matías I. Sancho and Virginia C. Aparicio performed the (UHPLC-MS/MS) analysis.
- Walter Massad and José Natera planned the different experiments and collaborated with the preparation of the manuscript.
- José Natera organized the final discussion and, wrote the manuscript.

All authors discussed on the results and commented on the manuscript. All authors have given approval to the final version of the manuscript

Declaration of interests

The authors declare that they have no known competing financial interests or personal relationships that could have appeared to influence the work reported in this paper.

Acknowledgments

Financial support from Consejo Nacional de Investigaciones Científicas y Técnicas (CONICET), Agencia Nacional de Promoción Científica y Tecnológica (ANPCyT), Secretarías de Ciencia y Técnica of the Universidad Nacional de Río Cuarto (SECyT UNRC).

REFERENCES

- [1] T. Zaugg, T. Hunziker, Germall II and Triclosan, Contact Dermatitis. 17 (1987) 262–262. <https://doi.org/10.1111/j.1600-0536.1987.tb02738.x>.
- [2] B. Steinkjer, L.R. Braathen, Contact dermatitis from triclosan (Irgasan DP 300), Contact Dermatitis. 18 (1988) 243–244. <https://doi.org/10.1111/j.1600-0536.1988.tb02815.x>.
- [3] D. Perrenoud, A. Bircher, T. Hunziker, H. Sutter, L. Bruckner-Tuderman, J. Stäger, W. Thürlimann, P. Schmid, A. Suard, N. Hunziker, Swiss Contact Dermatitis Research Group, Frequency of sensitization to 13 common

- preservatives in Switzerland *, *Contact Dermatitis*. 30 (1994) 276–279.
<https://doi.org/10.1111/j.1600-0536.1994.tb00597.x>.
- [4] M. Ricart, Triclosan persistence through wastewater treatment plants and its potential toxic effects on river biofilms, *Aqua Toxic*. 100 (2010) 346–353.
- [5] D.C. McAvoy, B. Schatowitz, M. Jacob, A. Hauk, W.S. Eckhoff, Measurement of triclosan in wastewater treatment systems, *Environ. Toxicol. Chem*. 21 (2002) 1323–1329. <https://doi.org/10.1002/etc.5620210701>.
- [6] K. Zeng, H. Hwang, Y. Zhang, H. Yu, Identification of 6-aminochrysene photoproducts and study of the effect of a humic acid and riboflavin on its photolysis, *J. Photochem. Photobiol. B*. 72 (2003) 95–100.
<https://doi.org/10.1016/j.jphotobiol.2003.09.006>.
- [7] B. Ertit Taştan, G. Dönmez, Biodegradation of pesticide triclosan by *A. versicolor* in simulated wastewater and semi-synthetic media, *Pestic. Biochem. Physiol*. 118 (2015) 33–37.
<https://doi.org/10.1016/j.pestbp.2014.11.002>.
- [8] C.A. Banassi, E. Scoffone, G. Galiazzo, G. Iori, Proflavine-sensitized photooxidation of tryptophan and related peptides, *Photochem. Photobiol*. 6 (2008) 857–866. <https://doi.org/10.1111/j.1751-1097.1967.tb09650.x>.
- [9] C.T. Anger, C. Sueper, D.J. Blumentritt, K. McNeill, D.R. Engstrom, W.A. Arnold, Quantification of Triclosan, Chlorinated Triclosan Derivatives, and their Dioxin Photoproducts in Lacustrine Sediment Cores, *Environ. Sci. Technol*. 47 (2013) 1833–1843. <https://doi.org/10.1021/es3045289>.
- [10] M. Allmyr, F. Harden, L.-M.L. Toms, J.F. Mueller, M.S. McLachlan, M. Adolfsson-Erici, G. Sandborgh-Englund, The influence of age and gender on

- triclosan concentrations in Australian human blood serum, *Sci. Total Environ.* 393 (2008) 162–167. <https://doi.org/10.1016/j.scitotenv.2007.12.006>.
- [11] T.E.A. Chalew, R.U. Halden, Environmental Exposure of Aquatic and Terrestrial Biota to Triclosan and Triclocarban, *JAWRA J. Am. Water Resour. Assoc.* 45 (2009) 4–13. <https://doi.org/10.1111/j.1752-1688.2008.00284.x>.
- [12] K. Bester, Fate of Triclosan and Triclosan-Methyl in Sewage Treatment Plants and Surface Waters, *Arch. Environ. Contam. Toxicol.* 49 (2005) 9–17. <https://doi.org/10.1007/s00244-004-0155-4>.
- [13] European Commission, Directorate General for Health & Consumers, Opinion on triclosan COLIPA n° P27., 2011. <http://bookshop.europa.eu/uri?target=EUB:NOTICE:NDAQ11002:EN:HTML> (accessed April 20, 2020).
- [14] I. Bellot, P. Mollinedo, R. Gemio, I. Morales, M. Moraes, Degradación de clorofenoles en soluciones sintéticas utilizando hongos H3, *Rev. Boliv. Quím.* 28 (2011) 102–105.
- [15] R.M. Pemberton, J.P. Hart, Electrochemical behaviour of triclosan at a screen-printed carbon electrode and its voltammetric determination in toothpaste and mouthrinse products, *Anal. Chim. Acta.* 390 (1999) 107–115. [https://doi.org/10.1016/S0003-2670\(99\)00194-4](https://doi.org/10.1016/S0003-2670(99)00194-4).
- [16] K. Aranami, Photolytic degradation of triclosan in freshwater and seawater, *Chemosphere.* 66 (2007) 1052–1056.
- [17] A. Paul, S. Hackbarth, E. Zwirnmann, B. Röder, C.E.W. Steimberg, Photosensitized generation of singlet oxygen and its quenching by humic

- substances, *Humic Subst. Mol. Details Appl. Land Water Conserv.* (2005) 99–116.
- [18] J.N. Chacon, J. McLearn, R.S. Sinclair, Singlet oxygen yields and radical contributions in the dye-sensitised photo-oxidation in methanol of esters of polyunsaturated fatty acids (oleic, linoleic, linolenic and arachidonic), *Photochem. Photobiol.* 47 (1988) 647–656. <https://doi.org/10.1111/j.1751-1097.1988.tb02760.x>.
- [19] C.M. Krishna, S. Uppuluri, P. Riesz, J.S. Zigler, D. Balasubramanian, A study of the photodynamic efficiencies of some eye lens constituents, *Photochem. Photobiol.* 54 (1991) 51–58. <https://doi.org/10.1111/j.1751-1097.1991.tb01984.x>.
- [20] E. Haggi, S. Bertolotti, N.A. García, Modelling the environmental degradation of water contaminants. Kinetics and mechanism of the riboflavin-sensitised-photooxidation of phenolic compounds, *Chemosphere.* 55 (2004) 1501–1507. <https://doi.org/10.1016/j.chemosphere.2004.01.016>.
- [21] S.E. Vastano, P.J. Milne, W.L. Stahovec, K. Mopper, Determination of picomolar levels of flavins in natural waters by solid-phase ion-pair extraction and liquid chromatography, *Anal. Chim. Acta.* 201 (1987) 127–133. [https://doi.org/10.1016/S0003-2670\(00\)85331-3](https://doi.org/10.1016/S0003-2670(00)85331-3).
- [22] H. Görner, Oxygen uptake after electron transfer from amines, amino acids and ascorbic acid to triplet flavins in air-saturated aqueous solution, *J. Photochem. Photobiol. B.* 87 (2007) 73–80. <https://doi.org/10.1016/j.jphotobiol.2007.02.003>.

- [23] M. Zhan, X. Yang, Q. Xian, L. Kong, Photosensitized degradation of bisphenol A involving reactive oxygen species in the presence of humic substances, *Chemosphere*. 63 (2006) 378–386.
<https://doi.org/10.1016/j.chemosphere.2005.08.046>.
- [24] F. Xu, X.-N. Song, G.-P. Sheng, H.-W. Luo, W.-W. Li, R.-S. Yao, H.-Q. Yu, Sunlight-mediated degradation of methyl orange sensitized by riboflavin: Roles of reactive oxygen species, *Sep. Purif. Technol.* 142 (2015) 18–24.
<https://doi.org/10.1016/j.seppur.2014.12.031>.
- [25] P.M. David Gara, G.N. Bosio, V.B. Arce, L. Poulsen, P.R. Ogilby, R. Giudici, M.C. Gonzalez, D.O. Mártire, Photoinduced Degradation of the Herbicide Clomazone Model Reactions for Natural and Technical Systems, *Photochem. Photobiol.* 85 (2009) 686–692. <https://doi.org/10.1111/j.1751-1097.2008.00467.x>.
- [26] D.M. Leech, M.T. Snyder, R.G. Wetzel, Natural organic matter and sunlight accelerate the degradation of 17 β -estradiol in water, *Sci. Total Environ.* 407 (2009) 2087–2092. <https://doi.org/10.1016/j.scitotenv.2008.11.018>.
- [27] P.F. Heelis, The photophysical and photochemical properties of flavins (isoalloxazines), *Chem. Soc. Rev.* 11 (1982) 15–39.
<https://doi.org/10.1039/CS9821100015>.
- [28] F. Wilkinson, W.P. Helman, A.B. Ross, Rate Constants for the Decay and Reactions of the Lowest Electronically Excited Singlet State of Molecular Oxygen in Solution. An Expanded and Revised Compilation, *J. Phys. Chem. Ref. Data.* 24 (1995) 663–677. <https://doi.org/10.1063/1.555965>.

- [29] Y. Barbieri, Photodegradation of bisphenol A and related compounds under natural-like conditions in the presence of riboflavin: Kinetics, mechanism and photoproducts, *Chemosphere*. 73 (2008) 564–571.
- [30] J. Natera, E. Gatica, C. Challier, D. Possetto, W. Massad, S. Miskoski, A. Pajares, N.A. García, On the photooxidation of the multifunctional drug niclosamide. A kinetic study in the presence of vitamin B2 and visible light, *Redox Rep.* 20 (2015) 259–266.
<https://doi.org/10.1179/1351000215Y.0000000010>.
- [31] C. Gambetta, W.A. Massad, A.V. Nesci, N.A. García, Vitamin B2-sensitized degradation of the multifunctional drug Evernyl, in the presence of visible light – microbiological implications, *Pure Appl. Chem.* 87 (2015) 997–1010.
<https://doi.org/10.1515/pac-2015-0407>.
- [32] W.A. Massad, S.G. Bertolotti, M. Romero, N.A. García, A kinetic study on the inhibitory action of sympathomimetic drugs towards photogenerated oxygen active species. The case of phenylephrine, *J. Photochem. Photobiol. B.* 80 (2005) 130–138. <https://doi.org/10.1016/j.jphotobiol.2005.03.010>.
- [33] S. Miskoski, N.A. García, Dark and photoinduced interactions between riboflavin and indole auxins, *Collect. Czechoslov. Chem. Commun.* 56 (1991) 1838–1849. <https://doi.org/10.1135/cccc19911838>.
- [34] C.S. Foote, Chemistry of Singlet Oxygen. XXI. Kinetics of Bilirubin Photooxygenation, *J Am Chem SOc.* 97 (1975) 6209–6214.
- [35] R.D. Scurlock, S.E. Braslavsky, K. Schaffner, A phytochrome study using two-laser/two-color flash photolysis: I700 is a mandatory intermediate in the PrPfr

- phototransformation, *Photochem. Photobiol.* 57 (1993) 690–695.
<https://doi.org/10.1111/j.1751-1097.1993.tb02939.x>.
- [36] E. Gatica, D. Possetto, A. Reynoso, J. Natera, S. Miskoski, E. De Geronimo, M. Bregliani, A. Pajares and W. A. Massad. Photo-Fenton and Riboflavin-photosensitized Processes of the Isoxaflutole Herbicide, *Photochem. Photobiol.* 95 (2019) 901–908. <https://doi.org/10.1111/php.13047>
- [37] C. Schweitzer, R. Schmidt, Physical Mechanisms of Generation and Deactivation of Singlet Oxygen, *Chem. Rev.* 103 (2003) 1685–1758.
<https://doi.org/10.1021/cr010371d>.
- [38] P. Wong-Wah-Chung, S. Rafqah, G. Voyard, M. Sarakha, Photochemical behaviour of triclosan in aqueous solutions: Kinetic and analytical studies, *J. Photochem. Photobiol. Chem.* 191 (2007) 201–208.
<https://doi.org/10.1016/j.jphotochem.2007.04.024>.
- [39] J.M. Buth, M. Grandbois, P.J. Vikesland, K. McNeill, W.A. Arnold, Aquatic photochemistry of chlorinated triclosan derivatives: Potential source of polychlorodibenzo-P-dioxins, *Environ. Toxicol. Chem.* 28 (2009) 2555–2563.
<https://doi.org/10.1897/08-490.1>.
- [40] T. Pluskal, S. Castillo, A. Villar-Briones, M. Orešič, MZmine 2: Modular framework for processing, visualizing, and analyzing mass spectrometry-based molecular profile data, *BMC Bioinformatics.* 11 (2010) 395.
<https://doi.org/10.1186/1471-2105-11-395>.
- [41] W.A. Massad, Y. Barbieri, M. Romero, N.A. Garcia, Vitamin B2-sensitized Photo-oxidation of Dopamine, *Photochem. Photobiol.* 84 (2008) 1201–1208.

- [42] C. Lu, W. Lin, W. Wang, Z. Han, S. Yao, N. Lin, Riboflavin (VB₂) photosensitized oxidation of 2'-deoxyguanosine-5'-monophosphate (dGMP) in aqueous solution: a transient intermediates study, *Phys. Chem. Chem. Phys. Inc. Faraday Trans. 2* (2000) 329–334. <https://doi.org/10.1039/A908492D>.
- [43] E. Haggi, S. Bertolotti, S. Miskoski, F. Amat-Guerri, N.A. García, Environmental photodegradation of pyrimidine fungicides — Kinetics of the visible-light-promoted interactions between riboflavin and 2-amino-4-hydroxy-6-methylpyrimidine, *Can. J. Chem.* 80 (2002) 62–67. <https://doi.org/10.1139/v01-192>.
- [44] R.M. Baxter, J.H. Carey, Evidence for photochemical generation of superoxide ion in humic waters, *Nature*. 306 (1983) 575–576. <https://doi.org/10.1038/306575a0>.
- [45] L.Y. Zang, H.P. Misra, Superoxide radical production during the autoxidation of 1-methyl-4-phenyl-2,3-dihydropyridinium perchlorate, *J. Biol. Chem.* 267 (1992) 17547–17552.
- [46] N.A. García, New trends in photobiology: Singlet-molecular-oxygen-mediated photodegradation of aquatic phenolic pollutants. A kinetic and mechanistic overview, *J. Photochem. Photobiol. B.* 22 (1994) 185–196. [https://doi.org/10.1016/1011-1344\(93\)06932-S](https://doi.org/10.1016/1011-1344(93)06932-S).
- [47] M.A. Sheraz, S.H. Kazi, S. Ahmed, Z. Anwar, I. Ahmad, Photo, thermal and chemical degradation of riboflavin, *Beilstein J. Org. Chem.* 10 (2014) 1999–2012. <https://doi.org/10.3762/bjoc.10.208>.

- [48] A.P. Darmanyan, C.S. Foote, Definition of the nature of ketone triplet states on the basis of singlet oxygen generation efficiency, *J. Phys. Chem.* 97 (1993) 4573–4576. <https://doi.org/10.1021/j100120a003>.
- [49] G. Porcal, S.G. Bertolotti, C.M. Previtali, M.V. Encinas, Electron transfer quenching of singlet and triplet excited states of flavins and lumichrome by aromatic and aliphatic electron donors, *Phys. Chem. Chem. Phys.* 5 (2003) 4123–4128. <https://doi.org/10.1039/B306945A>.
- [50] F.E. Scully, J. Hoigné, Rate constants for reactions of singlet oxygen with phenols and other compounds in water, *Chemosphere.* 16 (1987) 681–694. [https://doi.org/10.1016/0045-6535\(87\)90004-X](https://doi.org/10.1016/0045-6535(87)90004-X).
- [51] A.T. Soltermann, M. Luiz, M.A. Biasutti, M. Carrascoso, F. Amat-Guerri, N.A. García, Monosubstituted naphthalenes as quenchers and generators of singlet molecular oxygen, *J. Photochem. Photobiol. Chem.* 129 (1999) 25–32. [https://doi.org/10.1016/S1010-6030\(99\)00172-0](https://doi.org/10.1016/S1010-6030(99)00172-0).
- [52] E. Haggi, N. Blasich, J. Diaz, M. Diaz, W.A. Massad, F. Amat-Guerri, N.A. Garcia, Kinetics and Mechanism of the Sensitized Photodegradation of Uracil- Modeling the Fate of Related Herbicides in Aqueous Environments, *Photochem Photobiol.* 83 (2007) 520–525.
- [53] L. Fotouhi, H.R. Shahbaazi, A. Fatehi, M.M. Heravi, Voltammetric Determination of Triclosan in Waste Water and Personal Care Products, *Int J Electrochem Sci.* 5 (2010) 9.
- [54] M. Koizumi, S. Kato, N. Mataga, T. Matsuura, Y. Usui, *Photosensitized Reactions*, Kyoto, 1978.

- [55] D.R. Cardoso, K. Olsen, J.K.S. Møller, L.H. Skibsted, Phenol and Terpene Quenching of Singlet- and Triplet-Excited States of Riboflavin in Relation to Light-Struck Flavor Formation in Beer, *J. Agric. Food Chem.* 54 (2006) 5630–5636. <https://doi.org/10.1021/jf060750d>.
- [56] M. Díaz, M. Luiz, P. Alegretti, J. Furlong, F. Amat-Guerri, W. Massad, S. Criado, N.A. García, Visible-light-mediated photodegradation of 17 β -estradiol: Kinetics, mechanism and photoproducts, *J. Photochem. Photobiol. Chem.* 202 (2009) 221–227. <https://doi.org/10.1016/j.jphotochem.2008.12.008>.
- [57] J.R. Plimmer, U.I. Klingebiel, Riboflavin photosensitized oxidation of 2,4-dichlorophenol: assessment of possible chlorinated dioxin formation, *Science*. 174 (1971) 407–408. <https://doi.org/10.1126/science.174.4007.407>.
- [58] J. Al-Nu'airat, B.Z. Dlugogorski, X. Gao, N. Zeinali, J. Skut, P.R. Westmoreland, I. Oluwoye, M. Altarawneh, Reaction of phenol with singlet oxygen, *Phys. Chem. Chem. Phys.* 21 (2018) 171–183. <https://doi.org/10.1039/C8CP04852E>.

Compound	Solvent	${}^3k_q(\times 10^9)$ $M^{-1}s^{-1}$	$k_t(\times 10^8)$ $M^{-1}s^{-1}$	$k_r(\times 10^7)$ $M^{-1}s^{-1}$	k_r/k_t
TCS	MeOH-H ₂ O 1:1 v/v	0.58±0.04		0.13±0.02	0.087
	MeOD-D ₂ O 1:1 v/v		0.15±0.06		
	H ₂ O - 0.01 M NaOH			8.04±0.01	0.18
	D ₂ O - 0.01 M NaOH		4.5±0.4		
Phenol	MeOD		0.014 (a)		0.008
	H ₂ O (b)			0.00114(b)	
	H ₂ O, pH 10.3(c)		2.68	5	0.09
	MeOH (d)	0.48			
(a) [29](b) [58](c) [46]; (d) [20]					

Table 1. Rate constant values for the quenching of triplet excited state of Riboflavin by TCS (3k_q). Reactive (k_r) and overall (k_t) quenching rate constant of $O_2({}^1\Delta_g)$ by TCS and ratio k_r/k_t up on PN sensitized irradiation. Literature values for phenol were also included in the table for comparative purposes. Solvent: H₂O–MeOH, 1:1 v/v. k_t values were determined in D₂O–MeOD, 1:1 v/v solutions.

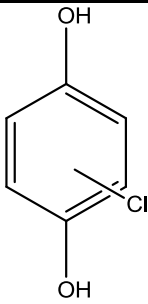
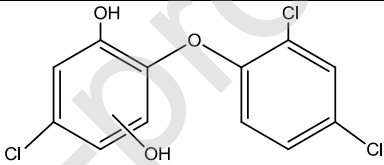
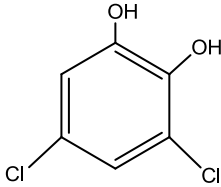
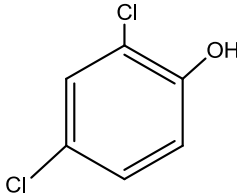
Peak N°/ Photolysis time	Retention time	m/z	Name
(1) /30 min	3.92 min	142	 Chlorohydroquinone
(4) / 30 min	4.80 min	303	 Monohydroxy-triclosan
(2) /60 min	4.36 min	177	 3,5-dichlorocatechol
(3) / 300 min	4.42 min	160	 2,4-dichlorophenol

Table 2. Retention time and m/z of the TCS degradation products using Rf as a sensitizer at different irradiation times.

SCHEME AND FIGURE CAPTIONS

Scheme 1: Possible pathways for the Rf-sensitized process in the presence of a hypothetical electron donor (TCS), which does not absorb at the irradiation wavelength. The overall rate constant involving both processes will be named k_t , being $k_t = k_r + k_q$, which accounts for the physical, k_q , and reactive, k_r , contribution to the overall deactivation, respectively.

Figure 1. Structures and absorption spectra of acid-base equilibrium of TCS (0,2 mM) species. (a): TCS in H₂O-MeOH 1:1v/v; (b): TCS in H₂O-MeOH 1:1v/v plus 10 mM NaOH.

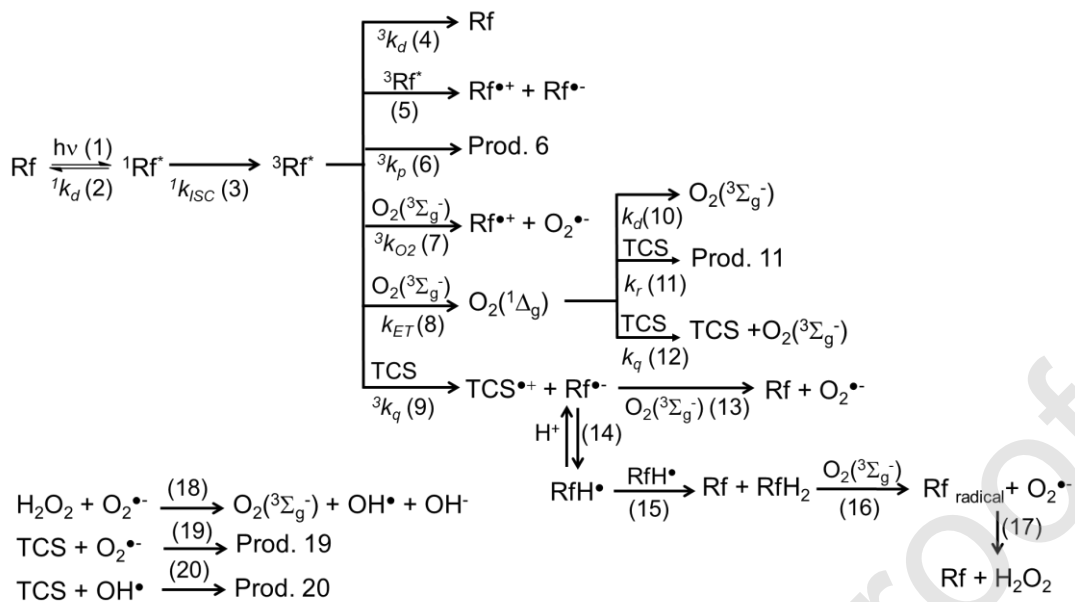
Figure 2. Changes in the UV-Vis difference absorption spectra in air equilibrated H₂O-MeOH 1:1 v/v solution of 0.035 mM Rf plus 0.1 mM TCS upon irradiation at 470 nm, taken vs. 0.035 mM Rf in the same solvent. Inset A: Changes in the UV-Vis difference absorption spectra of 0.035 mM Rf plus 0.1 mM TCS vs 0.035 mM Rf in Ar-saturated H₂O-MeOH 1:1 v/v solutions. Irradiation times for both figures: 0, 60, 120, 480, 2040 s. Inset B: absorbance decrease of TCS at 280 nm in air equilibrated (-■-) in Ar-saturated (-▶-).

Figure 3: Decay-associated spectra of Rf (0.05mM) in argon-saturated MeOH-H₂O 1:1 v/v in the absence (-■-) ³Rf* $\tau = 32 \mu\text{s}$, (-●-) RfH* $\tau = 490 \mu\text{s}$ and in the presence of TCS (-Δ-) ³Rf* $\tau = 5.6 \mu\text{s}$, (-◇-) RfH* $\tau = 280 \mu\text{s}$. Inset: Stern–Volmer

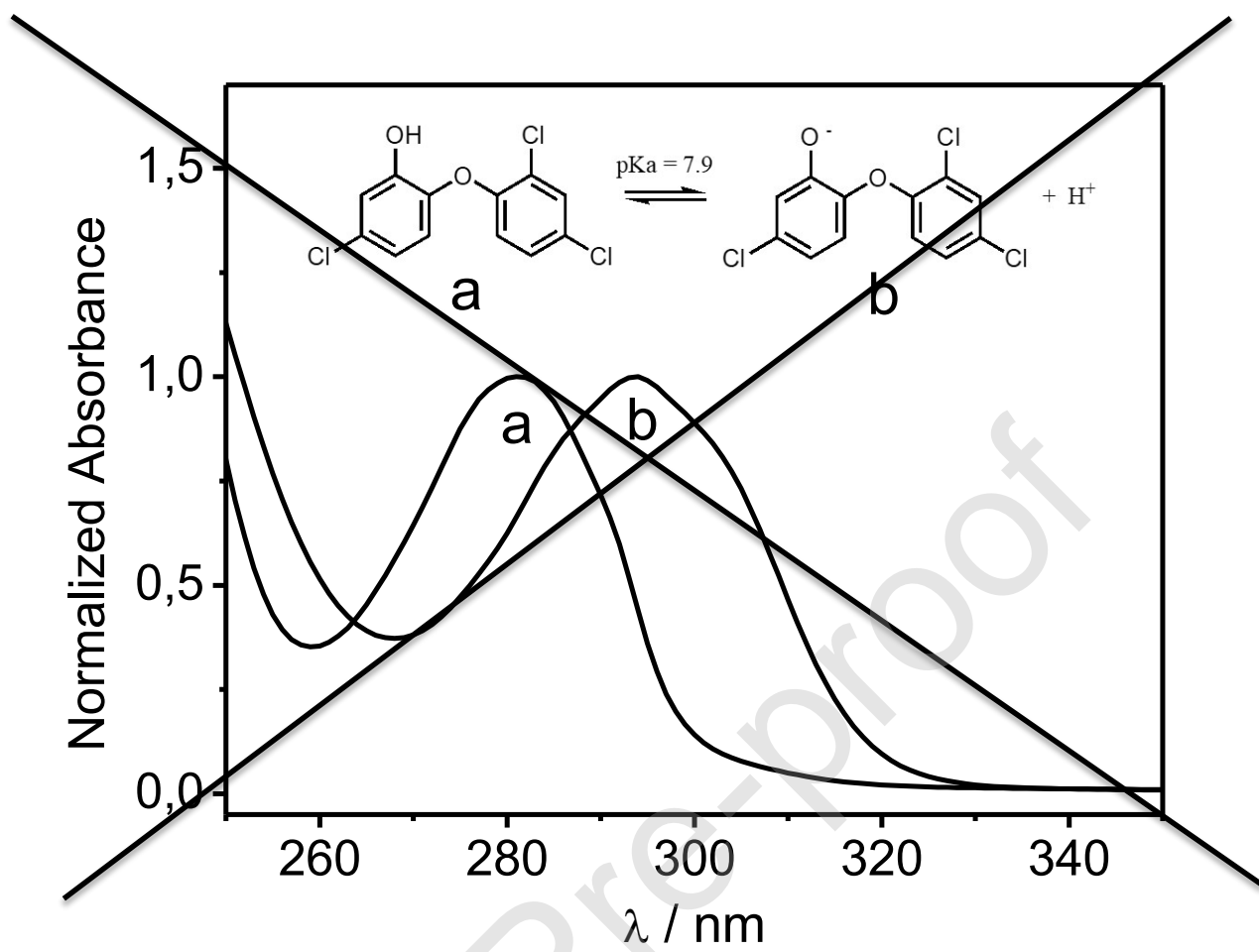
plot for the quenching of ${}^3\text{Rf}^*$ by TCS in MeOH-H₂O 1:1 v/v. τ_0 and τ refer to ${}^3\text{Rf}^*$ lifetimes in the absence and the presence of TCS, respectively. Error bars indicate one standard deviation.

445nm²

Figure 4. Stern–Volmer plots for the quenching of O₂(¹Δ_g) phosphorescence by TCS in D₂O solution plus 0.01 M NaOH (a) and MeOD-D₂O 1:1 v/v solution (b). Inset: first order plots for oxygen uptake in MeOH–H₂O 1:1 v/v solution containing PN + TCS (a), in aqueous solution plus 0.01 M NaOH (b) and MeOH–H₂O 1:1 v/v solution containing PN + FFA (c). [TCS] = [FFA] = 0.1 mM and PN as a sensitizer (A₃₆₃ = 0.5). Error bars indicate one standard deviations.



Scheme 1: Possible pathways for the Rf-sensitized process in the presence of a hypothetical electron donor (TCS), which does not absorb at the irradiation wavelength. The overall rate constant involving both processes will be named k_t , being $k_t = k_r + k_q$, which accounts for the physical, k_q , and reactive, k_r , contribution to the overall deactivation, respectively.



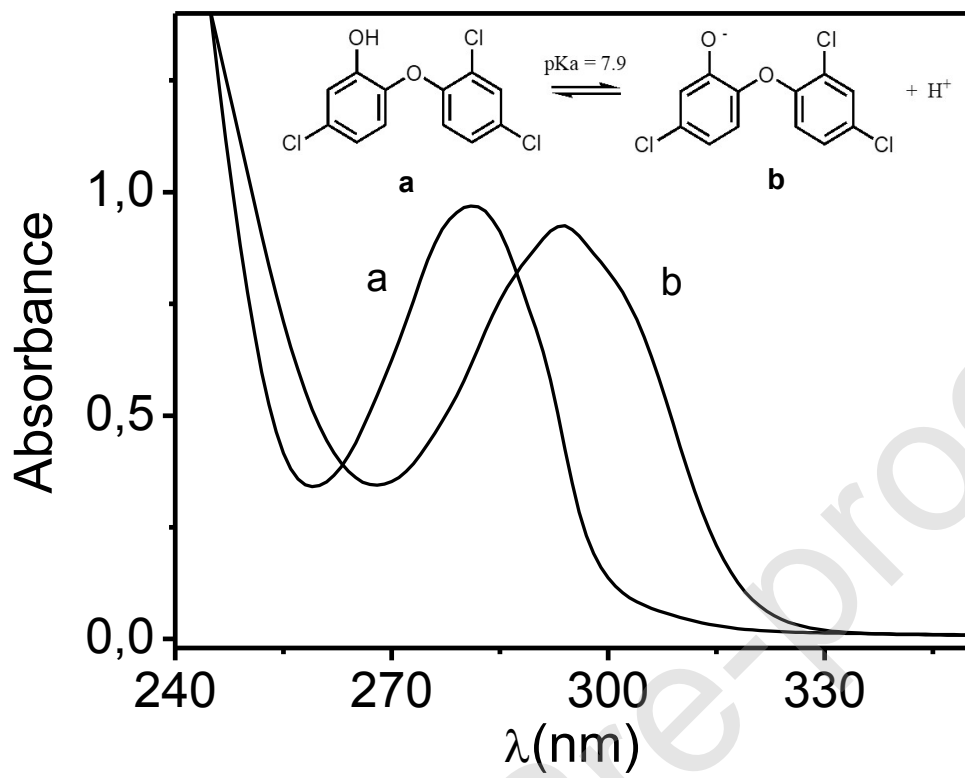
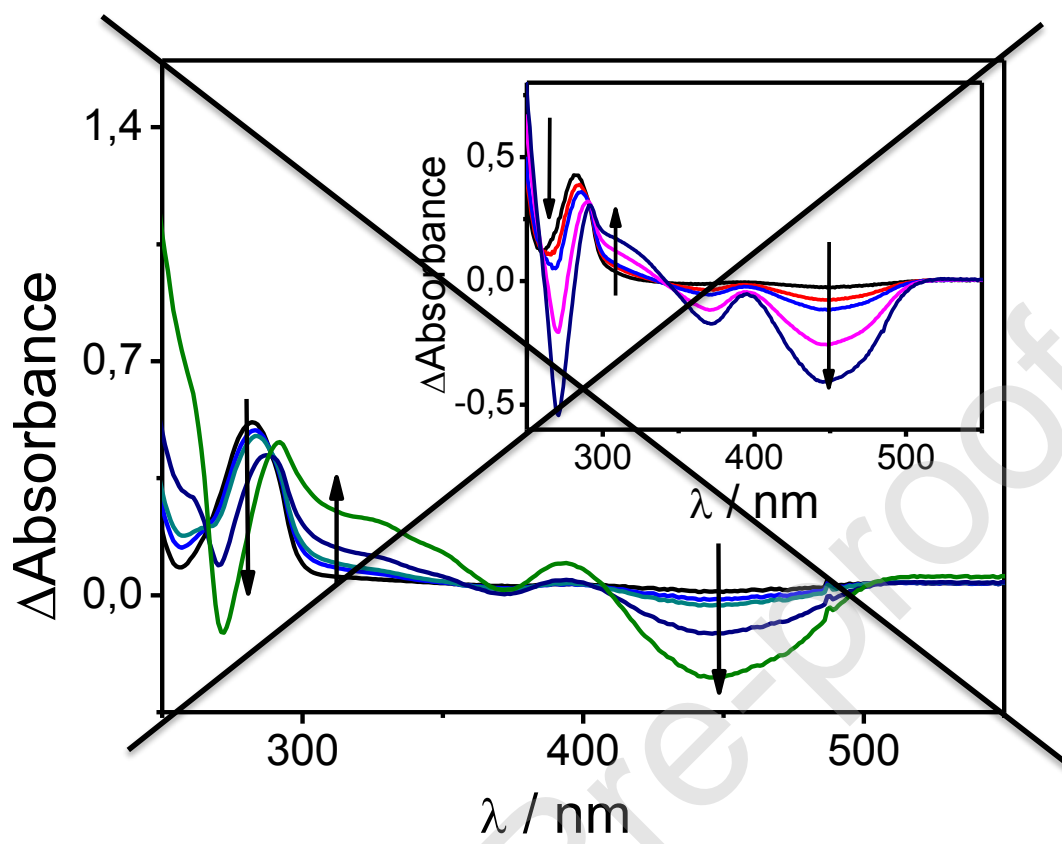


Figure 1. Structures and absorption spectra of acid-base equilibrium of TCS (0,2 mM) species. (a): TCS in H₂O-MeOH 1:1v/v; (b): TCS in H₂O-MeOH 1:1v/v plus 10 mM NaOH.



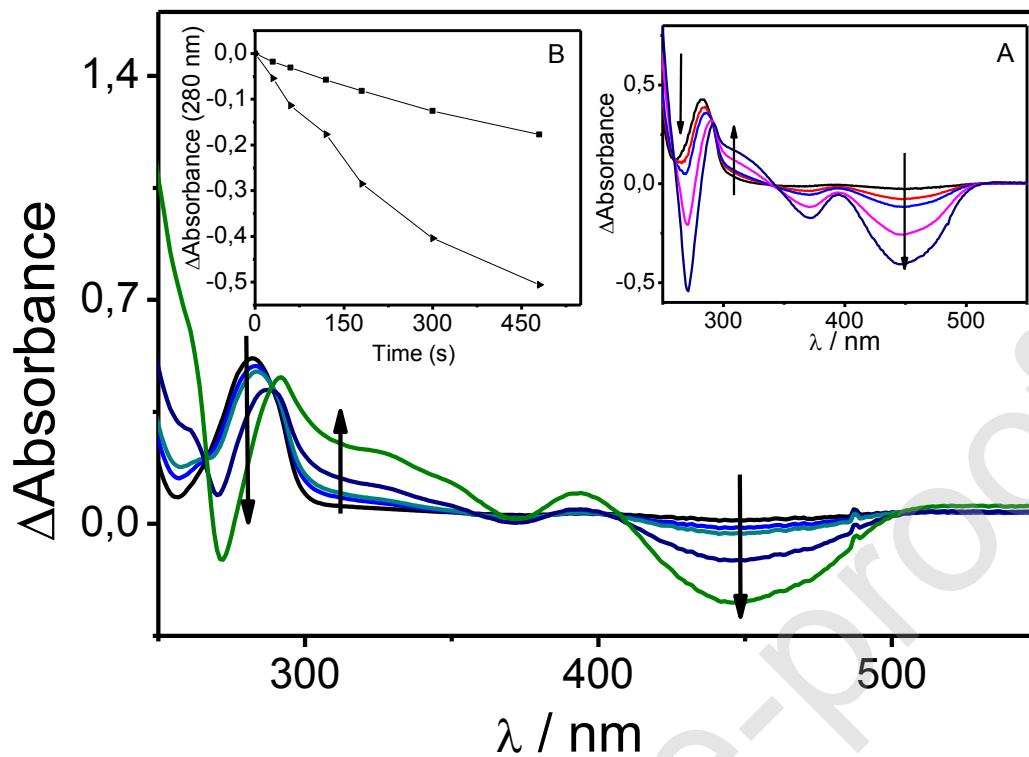


Figure 2. Changes in the UV-Vis difference absorption spectra in air equilibrated H₂O-MeOH 1:1 v/v solution of 0.035 mM Rf plus 0.1 mM TCS upon irradiation at 470 nm, taken vs. 0.035 mM Rf in the same solvent. Inset A: Changes in the UV-Vis difference absorption spectra of 0.035 mM Rf plus 0.1 mM TCS vs 0.035 mM Rf in Ar-saturated H₂O-MeOH 1:1 v/v solutions. Irradiation times for both figures: 0, 60, 120, 480, 2040 s. Inset B: absorbance decrease of TCS at 280 nm in air equilibrated (-■-) in Ar-saturated (-▶-).

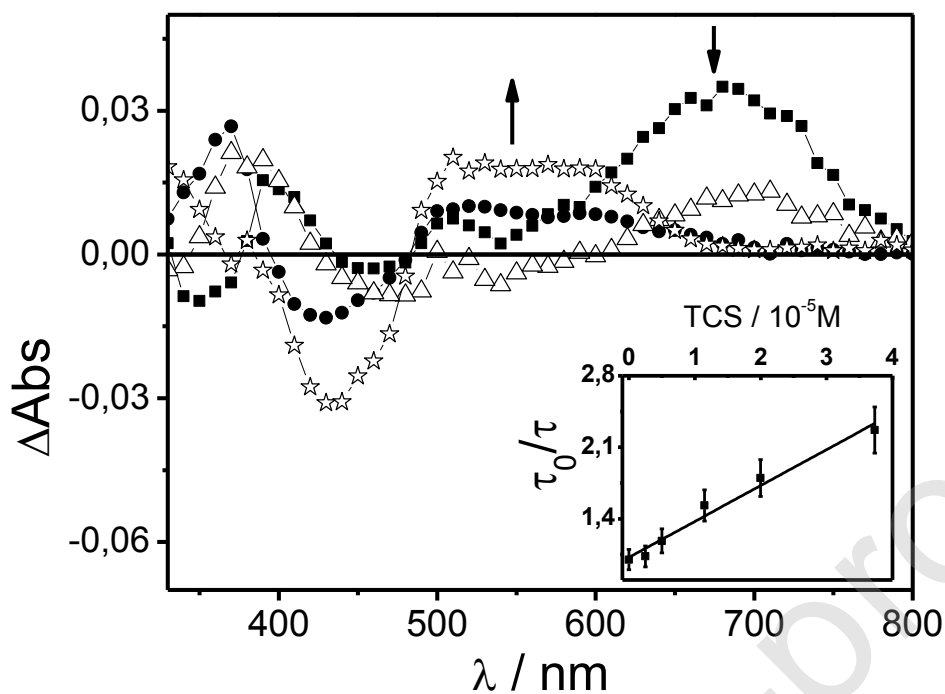
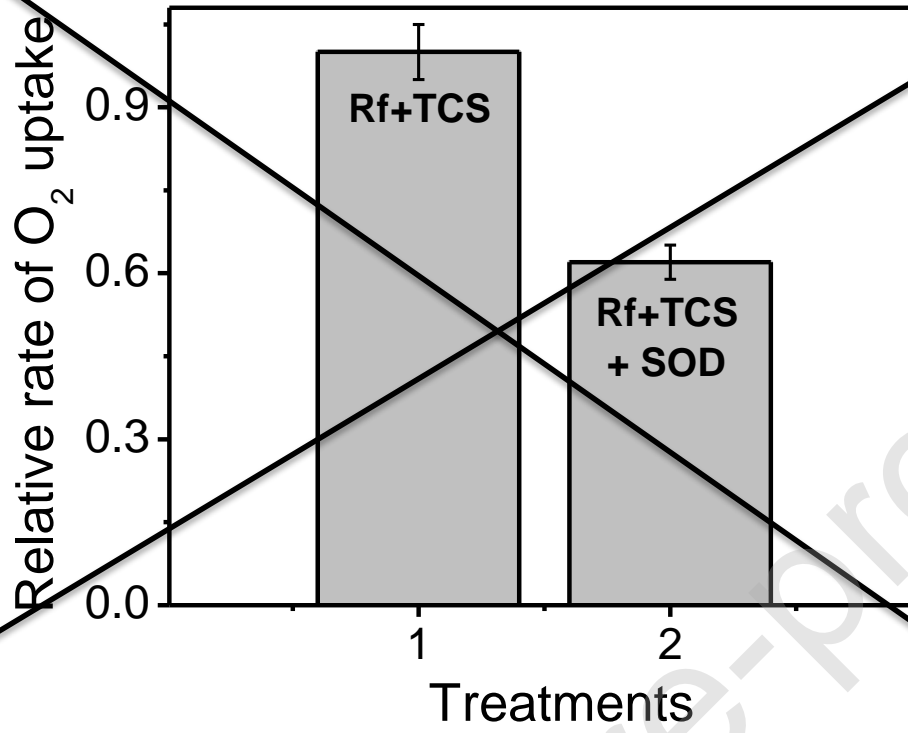


Figure 3: Decay-associated spectra of Rf (0.05mM) in argon-saturated MeOH-H₂O 1:1 v/v in the absence (-■-) $^3\text{Rf}^*$ $\tau = 32 \mu\text{s}$, (-●-) RfH^* $\tau = 490 \mu\text{s}$ and in the presence of TCS (-△-) $^3\text{Rf}^*$ $\tau = 5.6 \mu\text{s}$, (-◇-) RfH^* $\tau = 280 \mu\text{s}$. Inset: Stern–Volmer plot for the quenching of $^3\text{Rf}^*$ by TCS in MeOH-H₂O 1:1 v/v. τ_0 and τ refer to $^3\text{Rf}^*$ lifetimes in the absence and the presence of TCS, respectively. Error bars indicate one standard deviation.



445nm2

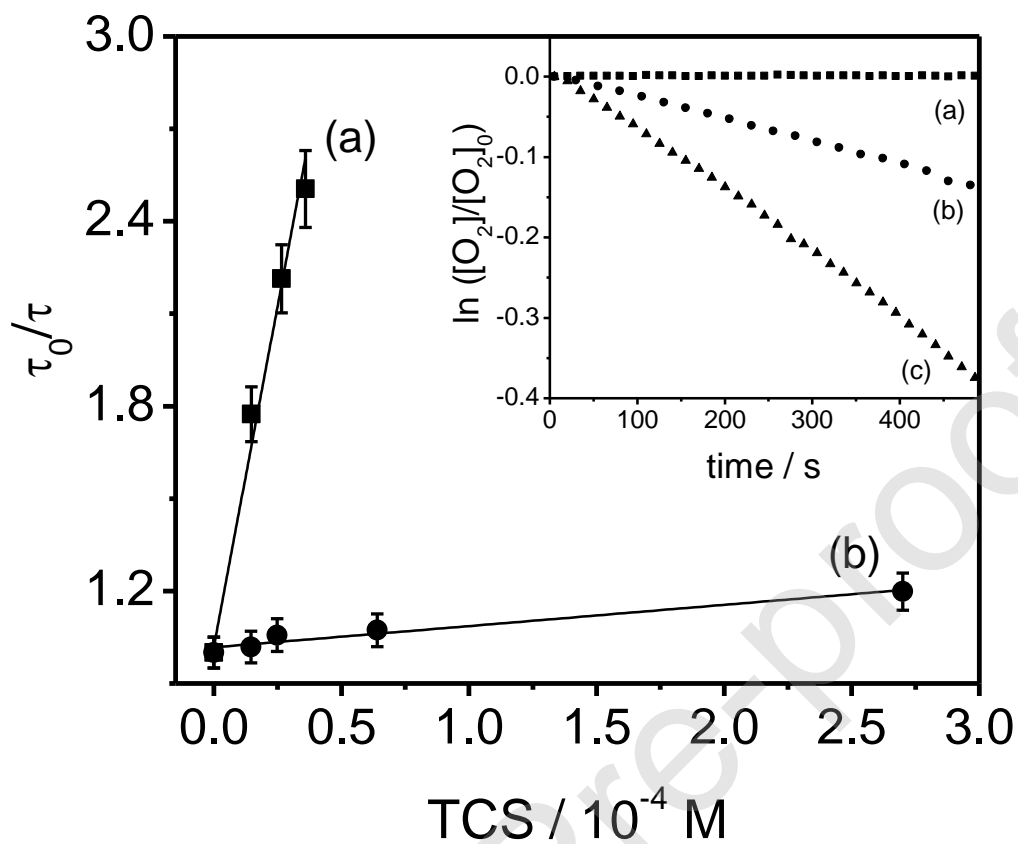


Figure 4. Stern–Volmer plots for the quenching of $O_2(^1\Delta_g)$ phosphorescence by TCS in D_2O solution plus 0.01 M NaOH (a) and MeOD- D_2O 1:1 v/v solution (b). Inset: first order plots for oxygen uptake in MeOH- H_2O 1:1 v/v solution containing PN + TCS (a), in aqueous solution plus 0.01 M NaOH (b) and MeOH- H_2O 1:1 v/v solution containing PN + FFA (c). $[TCS] = [FFA] = 0.1$ mM and PN as a sensitizer ($A_{363} = 0.5$). Error bars indicate one standard deviations.